DOI: 10.1002/ange.201305335

Polyamorphism

Low-Density Macroporous Foams Obtained from a Molecular Sieve by Temperature-Induced Amorphization**

*Stanislav Ferdov**

The thermal properties of zeolites and related porous solids are essential for their applications. It is currently thought that crystalline porous materials collapse to a dense amorphous state when subjected to temperatures above their thermal stability.[1,2] Herein, an alternative route of amorphization for ordered molecular sieves is revealed that leads to light, template-free, and hierarchical macroporous foams. Simple control of the time and temperature in an ambient atmosphere ensures thermal decomposition and drastic expansion of the microporous titanosilicate ETS-4 (Engelhard titanosilicate 4),[3] which results in progressively low-density (0.73–0.17 $g\,cm^{-3}$) multichamber bodies with pore sizes that range from less than one to several hundred micrometers. The formation of macroporous foams by thermal disintegration of crystalline microporous solids could be an ideal system for a better understanding of the amorphization phenomenon observed in molecular sieves, and offers a wide range of applications in the context of inorganic porous materials.

Porous crystalline materials comprise a large number of solids that are composed of condensed units of various elements. At elevated temperatures, their low-density frameworks compressively collapse to a glass with conventional density.[1] For a number of materials, this process of thermal amorphization is related to the co-existence of at least two amorphous phases with the same composition, but with different densities.[1,2,4–8] This phenomenon is known as polyamorphism[9,10] and is well-documented for tetrahedral microporous aluminosilicates, namely zeolites.[1,11–13] Polyamorphism in zeolites involves a low-density amorphous phase, which defines the onset of the structural collapse, and a high-density amorphous phase that forms later on further heating.[2] Similar to zeolites, transition-metal silicates show porous-network topologies, but instead of consisting of AlO_4 tetrahedra, the building blocks of the SiO_4 units are combined with MO_x polyhedra of various elements.[14] As a prominent member of that family, ETS-4 is a microporous titanosilicate that is known for its anticancer properties[15] and size-adjustable pores for gas separation.[16] The thermal behavior of ETS-4 has been studied profoundly,[16–19] and although the material has been known since the late 1980s,[3] nothing unusual about its amorphous state is reported. The structure starts to collapse at 200 °C, and it becomes completely amorphous at 500 °C. At higher temperatures (700–800 °C), the amorphous fraction transforms into a dense titanosilicate with narsarsukite structure.[18,20] Herein, we show how the thermal disintegration of ETS-4 reveals a route of amorphization that leads to macroporous structures with progressively expandable pores and low-density frameworks.

Macroporous titanosilicate foams were prepared by a one-step method. ETS-4 particles were gradually heated and cooled in air (for details, see the Experimental Section). The structural disintegration was followed by in situ powder X-ray diffraction; this was the first analysis to indicate a volumetric expansion of the growing foam (Figure S1).

Scanning electron microscopy (SEM) reveals that amorphization of ETS-4, which was realized up to 600 °C, preserved the integrity of initial crystal morphology (Figure 1 a). At 700 °C, the amorphous particles consolidate and drastically expand to a highly porous body (Figure 1 b, c). The vertical expansion amounts to more than 120 % of the initial bulk volume (Figure 1 d, e). The resulting density ($0.20 \pm 0.05\ g\,cm^{-3}$) is significantly lower than the crystallographic density ($2.35\ g\,cm^{-3}$) and the initial bulk density ($0.73 \pm 0.06\ g\,cm^{-3}$) of ETS-4 (Figure 2 a). The amorphous fractions

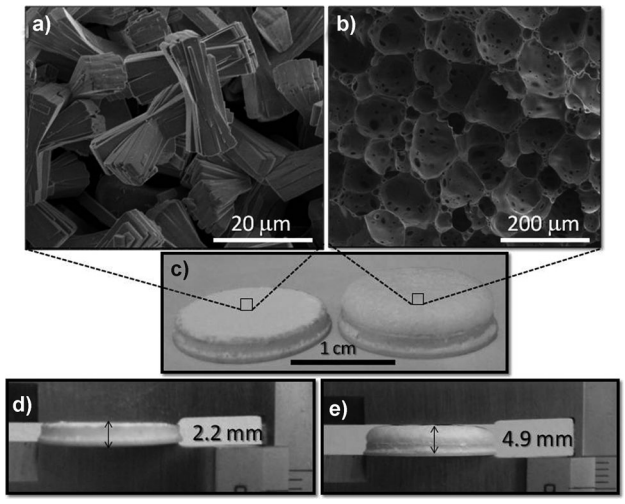

Figure 1. SEM and digital-camera images of temperature-amorphisized ETS-4. a) Shape-preserved particles of ETS-4 amorphisized at 600 °C; b) macroporous foam obtained after heating ETS-4 at 700 °C; c) corundum holder with ETS-4 after heating at 600 °C (left) and 700 °C (right); d) vertical expansion after heating ETS-4 at 600 °C and e) at 700 °C for 10 min.

[*] Dr. S. Ferdov
Department of Physics, University of Minho
Guimaraes 4800-058 (Portugal)
E-mail: sferdov@fisica.uminho.pt

[**] This work was supported by the Fundação para a Ciência e a Tecnologia (FCT) (PTDC/CTM/108953/2008 and NORTE-07-0124-FEDER-000037). The author also thanks SEMAT at the University of Minho for the XRD and SEM/EDS analyses.

Supporting information for this article is available on the WWW under http://dx.doi.org/10.1002/anie.201305335.

that were obtained at 600 °C and 700 °C showed a drastic difference in density, which indicates that the higher temperature leads to the formation of lighter glass (Figure 2a). When the change in molar volume is plotted versus the progress of the amorphization, it can be seen that the mechanism of amorphization for zeolites (FAU and LTA)[11] and metal–organic frameworks (ZIF-4)[21,22] is different than that for ETS-4 (Figure 2b). Instead of an overall decrease in molar volume, ETS-4 expands to a low-density framework upon heating, and a highly porous foam is formed; this result reveals a fundamentally new property of the family of molecular sieves. At 700 °C, the product of amorphization is composed of closely packed cells (Figure 3a) with a mean diameter of 63 μm and a size distribution of 20–120 μm (Figure 2c). The walls of the pores are decorated with a number of smaller (ca. 1–20 μm; secondary) openings, which provides a significant degree of hierarchy and a broad pore-size distribution.

An extended heating time, combined with an increase in temperature, allows the control of the density and porosity of the foams. When heated to 620, 640, 660, and 700 °C for 4 h, ETS-4 transforms into progressively lighter porous bodies with densities of 0.57 ± 0.04, 0.54 ± 0.05, 0.28 ± 0.03, and $0.17 \pm 0.05\ g\,cm^{-3}$, respectively (Figure 2a,d). The difference in density essentially originates from the size of the pores, which increases from low to high temperature (Figure 3b–d). At 620 °C, small bubbles reveal the onset of pore formation within the amorphous particles of ETS-4 (Figures 3b; Supporting Information, Figures S1a and S2). These pores have a narrow size distribution (ca. 0.2–2.4 μm) and a small average diameter (ca. 1 μm), and the initial morphological contour of the ETS-4 particles was preserved. At 640 °C, the process of pore formation is advanced, and the openings are larger with a doubled average pore diameter (ca. 2 μm; Figure 2c). The distribution of the pore size is narrow (ca. 0.5–4.5 μm), and no remnants that remind of the initial morphology of ETS-4 were observed (Figures 3c; Supporting Information, Figure S3). The foam openings are integrated in intergrowth tube-like bodies, which is indicative of a process of gradual cell coalescence. At 660 °C, the average diameter (47 μm) and the pore-size distribution (ca. 5–100 μm) significantly increase, and a foam of closely packed cells is formed (Figure 3d). The density is slightly higher than for the foam that was obtained at 700 °C with a heating time of 10 min (Figure 2a), but the surface of the pore walls is smooth, and no secondary openings are observed (Figure 3d). The foam that was heated at 700 °C for 4 h is crystalline (Figure 4a), with a pore network that is visible to the naked eye (Figure 4b). The collected powder XRD pattern is in good agreement with the diffractogram calculated for the dense titanosilicate narsarsukite $Na_2TiSi_4O_{11}$[20] (PDF: 033-1297). Considering that the narsarsukite and ETS-4 are not stoichiometrically equivalent, discrete amounts of secondary phases are also possible.[18] SEM images revealed pores with smeared contours (Figure 4c) and walls decorated with well-faceted pseudohexagonal crystals (Figure 4d,e). The average pore diameter (457 μm) is drastically larger than the one for the amorphous foams (Figure 2c), and the pore-size distribution (170–940 μm) is relatively narrow (Figure 4f). Although the

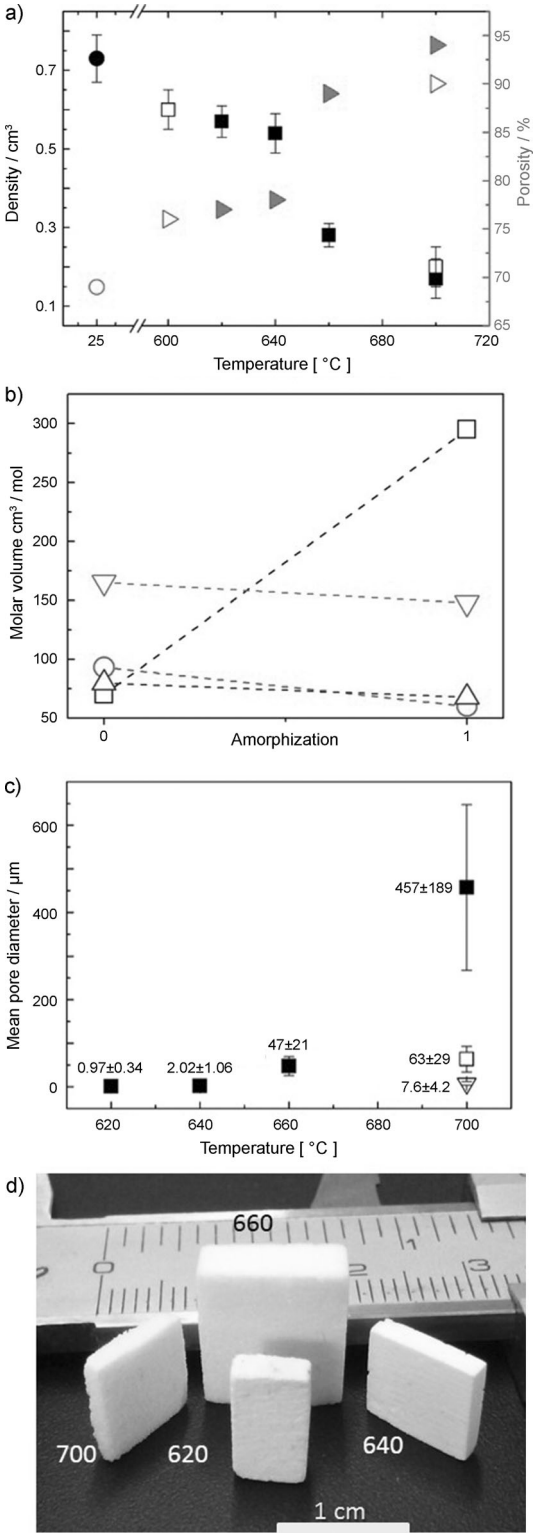

Figure 2. a) Effect of the temperature of amorphization on density and porosity, measured at room temperature (○ (porosity) and ● (density)), after heating for 10 min (□ (density) and ▷ (porosity)), and after heating for 4 h (■ (density) and ▶ (porosity)). b) Change in the molar volume with the amorphization process (0 crystalline; 1 completely amorphous) of ETS-4 (□), compared with zeolite Y (FAU;[11] ○), zeolite A (LTA;[11] △) and ZIF-4[22] (▽). c) Change in the average pore-size diameter of foams heated for 4 h (■); main pores of the foam obtained after heating for 10 min (□); and secondary pores of the foam obtained after heating for 10 min (▽). d) Digital-camera image of shaped foams that were obtained after heating at 620, 640, 660 (4 h), and 700 °C (10 min).

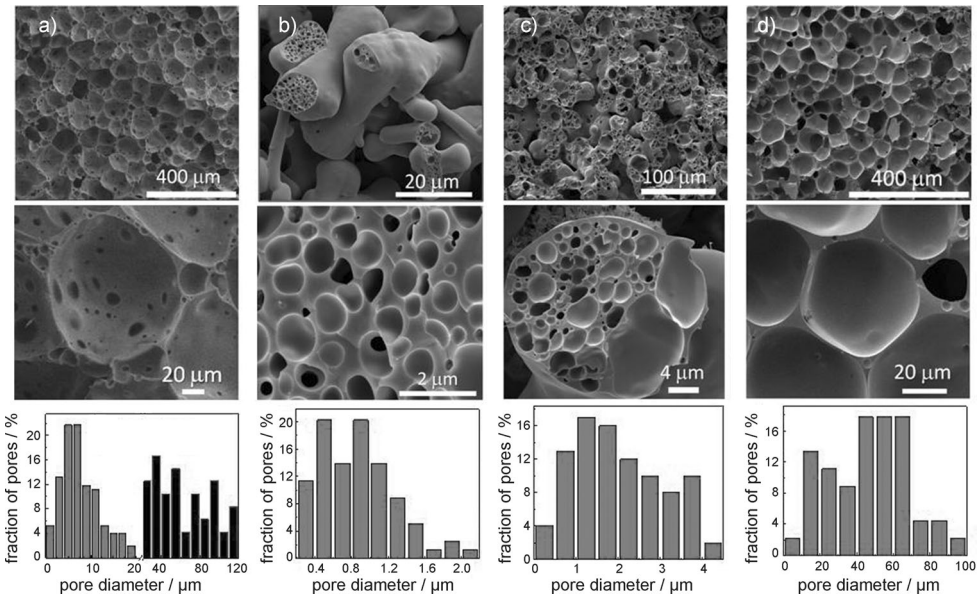

Figure 3. SEM images and statistical analysis of the pore-size distribution of foams that were obtained after heating at 700 °C for 10 min (a; left: secondary pores, right: main pores) and at 620 °C (b), 640 °C (c), and 660 °C (d) for 4 h. The relative standard deviations of all statistical data are 17.6% (main pores) and 13.7% (secondary pores; a), 13.9% (b), 10.6% (c), and 16.5% (d).

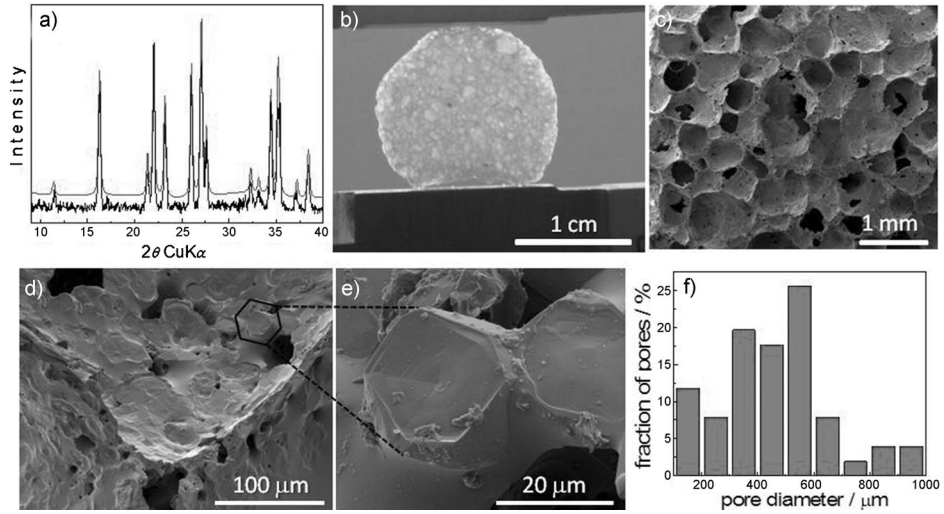

Figure 4. Calculated (——) and experimental XRD patterns (——; a), digital-camera (b) and SEM (c–e) images, and statistical analysis of the pore-size distribution (f) of macroporous foam composed of crystalline walls with a narsarsukite structure. The relative standard deviation of all statistical data is 17.6%.

crystallographic density of the narsarsukite (2.7 g cm^{-3}) is higher than the one of ETS-4, the large size of the bubbles ensures a very low density of the porous body (Figure 2a). Extending the heating time to up to 6 h or increasing the temperature to up to 800 °C led to a shapeless product with narsarsukite structure (Supporting Information, Figure S4).

Differential thermal analysis of ETS-4[18] indicates that the foaming temperature coincides with the temperature interval (ca. 620–700 °C) of a well-defined exothermic peak. This suggests that thermograms of other microporous materials can be used for predicting the temperature probably required for foam formation.

Our results reinforce the question as to why the transformation of ETS-4 into macroporous foams has not been observed thus far. A possible explanation entails that a proper combination of time and temperature of heating is required. When the sample is thermally amorphisized at the temperatures studied but for extended or shorter periods of time, ETS-4 was transformed into a dense titanosilicate narsarsukite or into amorphous particles that are not consolidated. Therefore, we suggest that it might be possible to obtain other foams based on silicate molecular sieve that occur at a certain stage of the thermal amorphization process. Thus, chemically and structurally new macroporous solids may be obtained by a process that avoids the use of expensive templates,[23] or by gas-bubbling[24] processes that are commonly needed to fabricate macroporous foams.

The self-foaming process introduced herein is based on a method that only entails heating in air for a short time. Thus, the fabrication should be easily scalable (Figure 2d), and hence applicable to larger-scale foam production at a low cost. Furthermore, the ability to swell and form bubbles when exposed to heat is well-known property of intumescent materials,[25] which makes ETS-4 a possible fire-retardant solid. In the context of known applications for inorganic macroporous materials, the prepared foams can potentially be used as low-weight structural and buoyant components (Figure S5), porous media for chemical and biological separation, catalyst supports, refractory filters for gases, scaffolds for tissue engineering, medical implants,[26] insulators, and systems for absorbing the kinetic energy from impacts.[27] In summary, our findings revealed polyamorphism in ordered molecular sieves that leads to progressively low-density amorphous phases as a result of the rising temperature.

Experimental Section

The amorphization of ETS-4 was performed in air with a heating rate of 0.5 °C s^{-1}. The sample was placed in a plate-like corundum holder and heated to a certain temperature (±1 °C) for 10 min or 4 h. The amorphization process was observed by in situ X-ray diffraction (XRD) analysis using the high-temperature chamber Anton Paar HTK 1200N that ensures a reliable measurement of the temperature.

The density of the foams was calculated from the sample weight (measured with a 5-digit analytical balance, AnD HR-120) divided by the volume of a regularly shaped sample. To determine the sample volume, three measurements of each dimension (by mechanical caliper and the digital micrometer Mitutoyo Absolute with a resolution of 0.001 mm) were made for two separate samples of the same foam. The density of the non-consolidated amorphous and crystalline particles (powder) was measured from the mass of a fixed volume by allowing particular packing. The porosity was calculated from the known actual, crystallographic, and pore-wall densities (assuming a glass density of 2.5 g cm^{-3}). The changes in the molar volume were calculated from the actual foam density and the known (crystallographic) density of ETS-4. The molar mass calculations were based on the formula of dehydrated ETS-4: $Na_{8.1}K_{0.9}Si_{12}Ti_5O_{38}$.

For each foam, the mean pore size and the pore-size distribution were calculated by measuring three principle cell diameters of 100 voids that were obtained by several SEM micrographs using the image analysis software *Image J* (NIH, Bethesda, Maryland, USA). Descriptive statistical analysis was used for describing the features of the collected data (pore frequency, mean values, and standard deviations).

Received: June 20, 2013
Revised: September 3, 2013
Published online: September 24, 2013

Keywords: amorphous materials · density · foams · molecular sieves · zeolites

[1] G. N. Greaves, F. Meneau, A. Sapelkin, L. M. Colyer, I. A. Gwynn, S. Wade, G. Sankar, *Nat. Mater.* **2003**, *2*, 622.
[2] A. Navrotsky, *Nat. Mater.* **2003**, *2*, 571.
[3] S. M. Kuznicki, US Patent 4853202, **1989**.
[4] Y. Katayama, T. Mizutani, W. Utsumi, O. Shimomura, M. Yamakata, K. Funakoshi, *Nature* **2000**, *403*, 170.
[5] O. Mishima, L. D. Calvert, E. Whalley, *Nature* **1985**, *314*, 76.
[6] H. W. Sheng, H. Z. Liu, Y. Q. Cheng, J. Wen, P. L. Lee, W. K. Luo, S. D. Shastri, E. Ma, *Nat. Mater.* **2007**, *6*, 192.
[7] P. F. McMillan, *J. Mater. Chem.* **2004**, *14*, 1506.
[8] P. F. McMillan, M. Wilson, D. Daisenberger, D. Machon, *Nat. Mater.* **2005**, *4*, 680.
[9] P. H. Poole, T. Grande, C. A. Angell, P. F. McMillan, *Science* **1997**, *275*, 322.
[10] E. G. Ponyatovsky, O. I. Barkalov, *Mater. Sci. Rep.* **1992**, *8*, 147.
[11] G. N. Greaves, F. Meneau, F. Kargl, D. Ward, P. Holliman, F. Albergamo, *J. Phys. Condens. Matter* **2007**, *19*, 415102.
[12] S. V. Goryainov, R. A. Secco, Y. Huang, H. Liu, *High Pressure Res.* **2006**, *26*, 395.
[13] G. N. Greaves, F. Meneau, O. Majerus, D. G. Jones, J. Taylor, *Science* **2005**, *308*, 1299.
[14] J. Rocha, M. W. Anderson, *Eur. J. Inorg. Chem.* **2000**, 801.
[15] S. Ferdov, E. Shikova, Z. Ivanova, L. T. Dimowa, R. P. Nikolova, Z. Lin, B. L. Shivachev, *RSC Adv.* **2013**, *3*, 8843.
[16] S. M. Kuznicki, V. A. Bell, S. Nair, H. W. Hillhouse, R. M. Jacubinas, C. M. Braunbarth, B. H. Toby, M. Tsapatsis, *Nature* **2001**, *413*, 652.
[17] S. Ferdov, *Langmuir* **2010**, *26*, 2684.
[18] M. Naderi, M. W. Anderson, *Zeolites* **1996**, *17*, 437.
[19] H. W. Xu, Y. P. Zhang, A. Navrotsky, *Microporous Mesoporous Mater.* **2001**, *47*, 285.
[20] D. R. Peacor, M. J. Buerger, *Am. Mineral.* **1962**, *47*, 539.
[21] T. D. Bennett, D. A. Keen, J. C. Tan, E. R. Barney, A. L. Goodwin, A. K. Cheetham, *Angew. Chem.* **2011**, *123*, 3123; *Angew. Chem. Int. Ed.* **2011**, *50*, 3067.
[22] J. T. Hughes, T. D. Bennett, A. K. Cheetham, A. Navrotsky, *J. Am. Chem. Soc.* **2013**, *135*, 598.
[23] A. Imhof, D. J. Pine, *Nature* **1997**, *389*, 948.
[24] G. T. Chandrappa, N. Steunou, J. Livage, *Nature* **2002**, *416*, 702.
[25] S. Bourbigot, M. Le Bras, S. Duquesne, M. Rochery, *Macromol. Mater. Eng.* **2004**, *289*, 499.
[26] U. T. Gonzenbach, A. R. Studart, E. Tervoort, L. J. Gauckler, *Angew. Chem.* **2006**, *118*, 3606; *Angew. Chem. Int. Ed.* **2006**, *45*, 3526.
[27] L. J. Gibson, M. F. Ashby, *Cellular Solids, Structure and Properties*, 2nd ed., Cambridge University Press, Cambridge, **1997**.